



Organic–inorganic hybrid superhydrophobic surfaces using methyltriethoxysilane and tetraethoxysilane sol–gel derived materials in emulsion

Xiu-Fang Wen*, Kun Wang, Pi-Hui Pi, Jin-Xin Yang**, Zhi-Qi Cai, Li-juan Zhang, Yu Qian, Zhuo-Ru Yang, Da-feng Zheng, Jiang Cheng

School of Chemistry and Chemical Engineering, South China University of Technology, Guangzhou 510640, PR China

ARTICLE INFO

Article history:

Received 12 May 2011

Received in revised form 16 June 2011

Accepted 16 June 2011

Available online 20 July 2011

Keywords:

Superhydrophobic surface

Organic–inorganic hybrids

Sol–gel process

MTES/TEOS

Hydrophobic silica

ABSTRACT

By applying alkaline-catalyzed co-hydrolysis and copolycondensation reactions of tetraethoxysilane (TEOS) and methyltriethoxysilane (MTES) in organic siloxane modified polyacrylate emulsion (OSPA emulsion), we are able to demonstrate the potential for developing a sol–gel derived organic–inorganic hybrid emulsion for a superhydrophobic surface research. TEOS and MTES derived sol–gel moieties can be designed for a physical roughness and hydrophobic characteristic (Si–CH₃) of the hybrid superhydrophobic surface, while OSPA emulsion can be endowed for good film-forming property. The effect of formulation parameters on superhydrophobicity and film-forming property was analyzed. The water contact angle (WCA) on the sol–gel derived hybrid film is determined to be 156°, and the contact angle hysteresis is 5° by keeping the mole ratio of TEOS:MTES:C₂H₅OH:NH₃·H₂O:AMP-95 at 1:4:30:10:0.63 and the mass percentage of OSPA emulsion at 25%. The nanoparticle-based silica rough surface is observed as the mole ratio of MTES/TEOS at 4:1. The sol–gel derived organic–inorganic hybrid emulsion shows remarkable film-forming property when the mole ratio of MTES/TEOS reaches or exceeds 4:1. With the primer coating, the performance of superhydrophobic film achieve actual use standard. It reveals that this new procedure is an effective shortcut to obtain a superhydrophobic surface with potential applications.

© 2011 Elsevier B.V. All rights reserved.

1. Introduction

Superhydrophobic surface can be prepared by a number of methods based on lithographic patterning [1,2], plasma etching [3], electrochemical deposition [4–8], chemical vapor deposition [9], sol–gel methods [10], layer-by-layer assembly plus phase separation [11,12], and utilization of templates. Among of them, sol–gel methods, especially which is based on organic-modified silica nano-particles, are one of the most common ways to be used to fabricate superhydrophobic surface with water contact angle (WCA) larger than 150° [13–17]. Those superhydrophobic surfaces were resulted from roughness based on the nanoparticle size and hydrophobic characteristic of organic moiety. The organic-modified materials included low surface-free-energy polybenzoxazine and fluoroalkylsilane, etc. For example, Nakajima et al. [18] created hard super-hydrophobic thin films by

combining a phase separation of tetraethyl orthosilicate (TEOS) induced by the addition of an acrylic polymer, and subsequent fluoroalkylsilane (FAS) coating. The film obtained by proper composition possessed high transmittance in the visible wavelength range and its hardness was almost at the same level as normal silica-based hard coatings. Ming et al. [19] prepared a superhydrophobic surface by synthesizing silica-based raspberry-like particles and binding them on an epoxy-based polymer matrix after surface modified with a layer of PDMS. Tsai and Lee [20] fabricated a superhydrophobic surface with advancing and receding WCAs of 169° and 165° on the dual size structured surface is by means of layer-by-layer assembly of silica particles modified by dodecyltrichlorosilane. Bravo et al. [21] demonstrated a layer-by-layer processing scheme that could be utilized to create transparent superhydrophobic surfaces from SiO₂ nanoparticles with various sizes. Transparent superhydrophobic films were created by the sequential adsorption of silica nanoparticles and poly (allylamine hydrochloride). The final assembly was rendered superhydrophobicity with trichloro (1H, 1H, 2H, 2H-perfluorooctyl) silane deposited by chemical vapor deposition (CVD). However, all above organic-modified hydrophobic films limited their applications due to their complicated organic reac-

* Corresponding author. Tel.: +86 20 87112057x805; fax: +86 20 87112057x804.

** Corresponding author. Tel.: +86 15902083578; fax: +86 20 87112057x804.

E-mail addresses: xfwen@scut.edu.cn (X.-F. Wen), jinxiny_2003@yahoo.com.cn (J.-X. Yang).

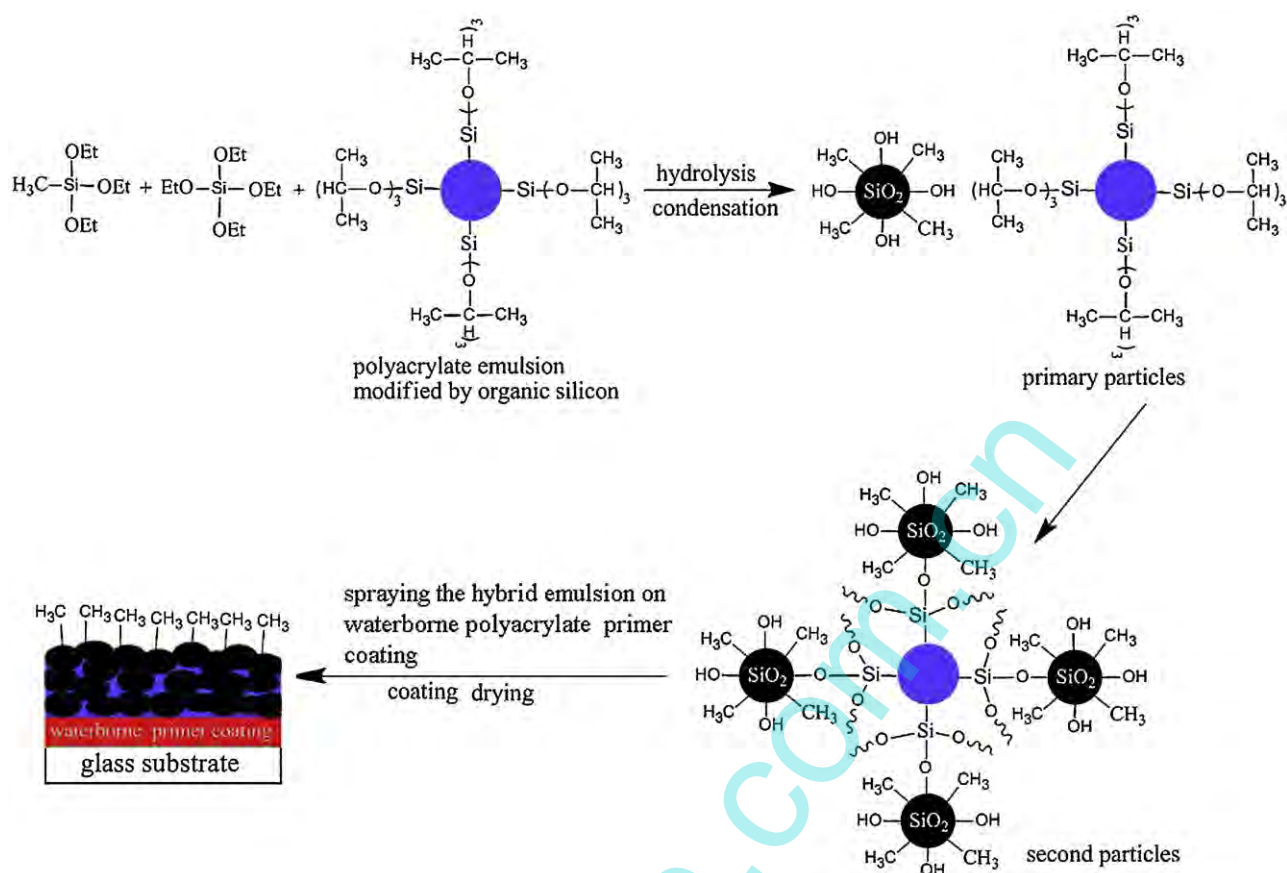


Fig. 1. Schematic illustration of sol-gel derived organic-inorganic hybrid coatings.

tions on nanoparticles and sophisticated experimental skills to control the surface characteristics and film performance. Also, the organic-modified materials including fluoro-materials were expensive, making it difficult to scale up the production for practical.

In this research work, superhydrophobic surfaces prepared through the sol-gel derived organic-inorganic hybrid emulsion were explored, as shown in Fig. 1. Firstly, the sol-gel derived organic-inorganic hybrid emulsion was created by alkaline-catalyzed co-hydrolysis and copolycondensation reactions of tetraethoxysilane (TEOS), methyltriethoxysilane (MTES) and tri(isopropoxy)vinylsilane (TIPVS) in OSPA emulsion. Sol-gel reaction on different compositions of MTES/TEOS/TIPVS was carried out to form the primary particles in suit in OSPA emulsion, the sol-gel derived organic-inorganic hybrid emulsion was obtained by the secondary particle in emulsion, which resulted from the further gelation on the above reaction product by adding ammonia. Finally, the above sol-gel derived organic-inorganic hybrid emulsion was sprayed onto the waterborne polyacrylate primer coating or glass substrate and dried at 110 °C for 2 h to form the superhydrophobic surfaces. TEOS derived silica was designed for a physical roughness of micro- and nano-scale binary structures, the character of the sol-gel derived hybrid film surface shifts from hydrophilic to superhydrophobic due to the incorporation of CH₃ groups in the silica surface with the help of MTES as the hydrophobic reagent. Film-forming properties were improved to enhance the strength of film cohesion with OSPA emulsion. The experimental results suggest that such simple non-fluoroalkyl silica could produce superhydrophobic surface with remarkable film property.

2. Experimental

2.1. Fabrication of OSPA emulsion

Emulsion polymerization was performed following a typical recipe: deionized water 69.6 g, A nonylphenol poly (oxyethylene) nonionic surfactant (OP-10), a reactive anionic surfactant (DNS-86, allyloxy polyoxyethylene (10) nonyl ammonium sulfate) were used as emulsifier at 0.4 g (OP/DNS-86 = 1/1 wt) was transferred into a thermostated reactor with continuous stirring. After the mixture was stirred for 1 h, the mixture monomer of 13.5 g methyl methacrylate (MMA), 13.8 g butyl acrylate (BA), 1.2 g hydroxyethyl methacrylate (HEMA), and 1.5 g TIPVS and potassium persulfate (KPS) were added. The polymerization started at 75 °C and finished within 2 h. A stable OSPA emulsion can be obtained to cool the reaction liquid below 40 °C when the reaction was kept for 6 h. It was necessary to control the pH value of initial dispersion (about pH 7–7.5) by using a NaHCO₃ buffer to control the hydrolysis of TIPVS.

2.2. Preparation of sol-gel derived organic-inorganic hybrid emulsion

10 g OSPA emulsion (30 wt%) was introduced in a 100 mL, three-neck, round-bottom flask equipped with a heat exchange system. 22.36 g absolute ethyl alcohol, 4.52 g 2-Amino-2-methyl-1-propanol, 11.56 g MTES and 3.38 g TEOS were added and the reactive solution was stayed stirring for 1 h at room temperature. Then 4.52 g ammonia was added under stirring at room temperature for 6 h and sol-gel derived organic-inorganic hybrid emulsion was obtained. The size and structure of silica/polymer composite

particles could be controlled by changing the mole ratio of MTES and TEOS and the weight ratio of sol–gel derived SiO₂ particle to latex.

2.3. Characterization

The morphologies of hybrid emulsion particles were investigated by transmission electron microscopy (TEM, Tecnai 10, Philips Corporation, Holand), microscope at accelerating voltage of 100 kV. One drop of emulsion was diluted by amount of water and placed on a carbon-coated copper grid and dried in air before observation. The surface morphologies of the particulate films were examined by scanning electron microscope (SEM, supplied by LEO (LEO 1530VP)) and Atomic Force Microscopy (AFM, performed on a Dimension 62,000 nm instrument (CSPM2000)). AFM images were acquired under ambient conditions in tapping mode using a Nanoprobe cantilever. WCA of the surface was measured with an OCA15 contact angle goniometer from Dataphysics Co. Germany. Typically, the average value of five measurements, made at different positions of the film surface was adopted as the value of WCA. FT-IR was used to study the chemical composition of powder samples and hybrid emulsion film sample. The KBr pellet technique was used to prepare the powder samples, hybrid emulsion film sample was prepared by spraying the hybrid emulsion on tinplate. FT-IR (Vector 33, Bruker Corporation, Germany) was operated in the 4000–400 cm⁻¹ range and the average of three scans for each sample was taken for the peak identification. ²⁹Si solid-state NMR was recorded at room temperature using a Bruker AM 400 spectrometer. The sample was ground to a fine power and then placed into the NMR tube.

2.4. Test method of basic performances of film

Impact resistance of film was examined according to the Chinese national standard of GB/T-1732-93, which is defined to detect the maximum height which the free falling 1000 g counter weight would not destroy the film on the tinplate. The analysis of adhesive attraction was conducted according to adhesive attraction test methods in GB/T9286-1998. According to that national standard, the blade is used to cut the film to make lattice pattern on the film, with the number of both horizontal and vertical cuts being 6 in every cutting graph. The result is grade 2 when a cross-cut area distinctly greater than 5%, but not distinctly greater than 15% is affected. The test will be executed at least three times on one sample. Hardness was also examined to detect the hardest grade pencil that the film would not be scraped by pencil according to the Chinese national standard of GB/T6739-1996. The pencil used in our experiment is Zhonghua brand advanced drawing pencil.

Acid resistance, Alkali resistance and salt water resistance of film were evaluated by immersion of film into 3 wt% H₂SO₄, NaOH and NaCl aqueous solution, respectively. Check and evaluate the film appearance and superhydrophobicity renewing property after 48 h for H₂SO₄ and NaOH, and 7 days for salt water.

3. Results and discussion

3.1. ²⁹Si solid-state NMR and FT-IR studies

Fig. 2 exhibits the solid-state ²⁹Si NMR spectra of the MTES/TEOS sol–gel derived hybrid emulsion with the mole ratio of MTES/TEOS at 0:1, 1:1, 4:1, 1:0. The chemical shifts of silicon atoms with 0, 1, 2, 3 or 4 siloxane bridge are denoted as Q⁰, Q¹, Q², Q³, or Q⁴ [22]. As shown in Fig. 2, Q² and Q³ of MTES derived materials are observed at –52.6 and –60.8, Q³ and Q⁴ of TEOS derived materials are observed at –95.4, and –105.9, which are similar to those

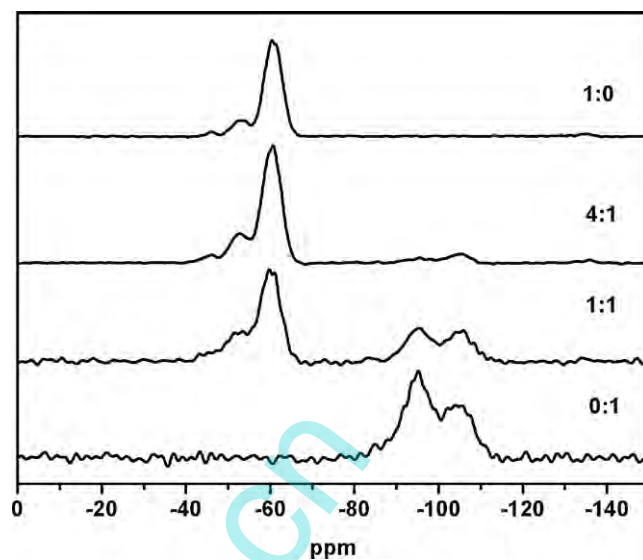


Fig. 2. Solid-state ²⁹Si NMR spectra of the sol–gel derived organic–inorganic hybrid emulsion with different MTES/TEOS compositions.

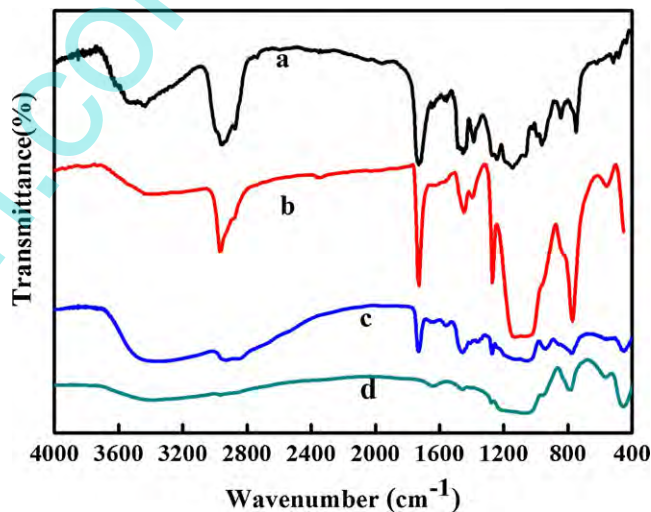


Fig. 3. FT-IR of OSPA (a), sol–gel derived organic–inorganic hybrid emulsion film on tinplate (b), sol–gel derived organic–inorganic hybrid emulsion (KBr pellet technique) (c) and MTES/TEOS hybrid silica sols (d).

reported in the literature [22,23]. The peak intensities of Q² and Q³ of MTES derived materials increase with increasing the MTES mole ratio while Q³ and Q⁴ peak intensities of TEOS derived materials show a reverse trend. It can be deduced that the synthesized materials compositions are similar to those of the feeding mole ratio of MTES/TEOS.

The MTES/TEOS sol–gel derived organic–inorganic hybrid emulsion composition was further characterized by FT-IR. Curve a, b, c and d in Fig. 3 are the FT-IR spectrum curve of OSPA emulsion, sol–gel derived organic–inorganic hybrid emulsion film on tinplate, sol–gel derived organic–inorganic hybrid emulsion (KBr pellet technique) and MTES/TEOS hybrid silica sols, respectively. For curve a, the peak at 2800–3000 cm⁻¹ is due to the C–H (CH₂) of polyacrylate, the peak at 1732 cm⁻¹ corresponds to the C=O stretching vibration, the peaks at 1454 cm⁻¹ and 1387 cm⁻¹ are due to in-plane symmetric flexural vibrations absorption peaks and asymmetric flexural vibrations absorption peaks of the –CH₃. The peak at 3300–3500 cm⁻¹ is due to water and OH group.

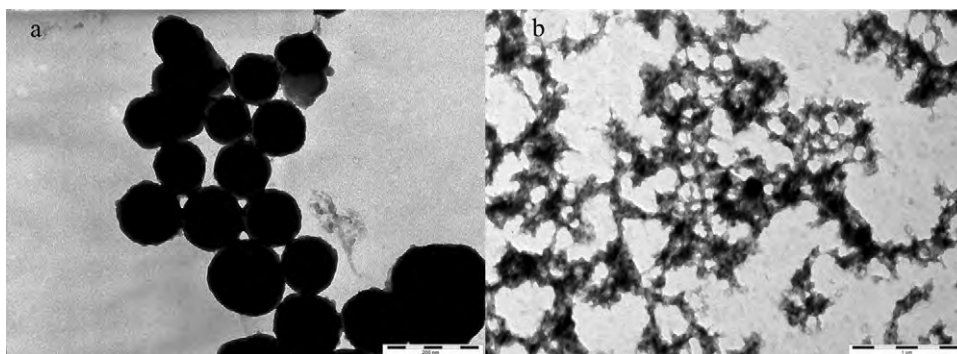


Fig. 4. TEM of silica sol (a) and organic–inorganic hybrid materials (b).

Considering the disappearance of peak at 1640 cm^{-1} , there is no free monomer in the OSPA emulsion. For curve d, the wide absorption peaks of OH at 3435 cm^{-1} and 1638 cm^{-1} is contributed to the water molecular, OH group of ethyl alcohol and unreacted the hydroxyl groups in modified SiO_2 . The dramatic reduction of intensity of absorption peak at $2800\text{--}3000\text{ cm}^{-1}$ indicates that the hydrolysis reaction of the mixture of TEOS and METS is complete. The peak of 1276 cm^{-1} is the character absorption peaks of Si-CH_3 , the peaks at $1100\text{ cm}^{-1}\text{--}1200\text{ cm}^{-1}$ interval and 459 cm^{-1} are contributed to the symmetric stretching vibration absorption peaks and asymmetric stretching vibration absorption peaks of Si-O-Si [23]. This pattern is indicated that it is the sol–gel derived materials of MTES/TEOS. Comparing curve b and c to a and d, the FT-IR spectrum of sol–gel derived organic–inorganic hybrid emulsion film on tinplate and sol–gel derived organic–inorganic hybrid emulsion (KBr pellet technique) had all the characteristic bands of MTES/TEOS hybrid silica sols and OSPA latex, curve b is more similar to curve a and curve c is more similar to curve d, it suggested that OSPA is the film-forming substance, and can fasten the SiO_2 particles in polymer network.

3.2. Transmission electron microscopy

The morphology of MTES/TEOS hybrid silica sols and sol–gel derived organic–inorganic hybrid emulsion particle were characterized by TEM and the results are shown in Fig. 4. It can be seen from Fig. 4a that MTES/TEOS hybrid silica sols are sphericity. However, the size and distribution of SiO_2 particles were non-uniform due to using the mixture of MTES and TEOS as precursor. The reason is that tetra-functional TEOS sol–gel reaction generally exhibits a three-dimension microstructure with hydrophilic OH groups on the surfaces, the tri-functional MTES may have a two-dimension planar structure with hydrophobic CH_3 groups on the silica surfaces [24]; sol–gel process was affected by the Si-CH_3 of MTES in our experiment. When sol–gel precursor solution was introduced

into polyacrylate emulsion, the polymer emulsion particles were embedded by inorganic SiO_2 particles and the morphology of polymer emulsion particles and inorganic SiO_2 particles was changed to be irregular (Fig. 4b). This is in favor of film forming and improving the film properties.

3.3. Atomic force microscopy (AFM)

The wettability of surface is dependent not only on its chemical composition, but also on the topography of surface. Fig. 5a and b show the typical three dimensional AFM images of OSPA emulsion film surface and sol–gel derived organic–inorganic hybrid emulsion film surface. The results of preliminary quantitative analysis, such as root-mean-square roughness (Sq which gives the standard deviation of the height values), surface roughness factor (r , $r = 1 + Sdr$, Sdr is surface area ratio, which is the ratio between the interfacial and projected areas) and mean roughness (Ra), were obtained from AFM software analysis in Table 1. For the film of OSPA emulsion, the smooth film surface appears to be featureless and the roughness factor is 1.006 and Sq is 7.05 nm (Fig. 5a). For the sol–gel derived organic–inorganic hybrid film, the roughness factor is 10.6, Sq is 202 nm (Fig. 5b). The water contact angle is increased to 156° , and the contact angle hysteresis decreases to 5° . The surface roughness is increased due to inorganic SiO_2 introduced. It is as expected that sol–gel derived organic–inorganic hybrid film has a higher contact angle than the film of OSPA emulsion because of higher roughness.

3.4. Film property measurements

Organic–inorganic hybrid superhydrophobic film with remarkable performance was obtained by spraying the hybrid emulsion on waterborne polyacrylate primer coating (Apose company, Zhongshan, Guangdong) and then drying it at 110°C for 2 h. The performance of superhydrophobic coating and the cross-section of hybrid film with primer coating are shown in Table 2 and Fig. 6.

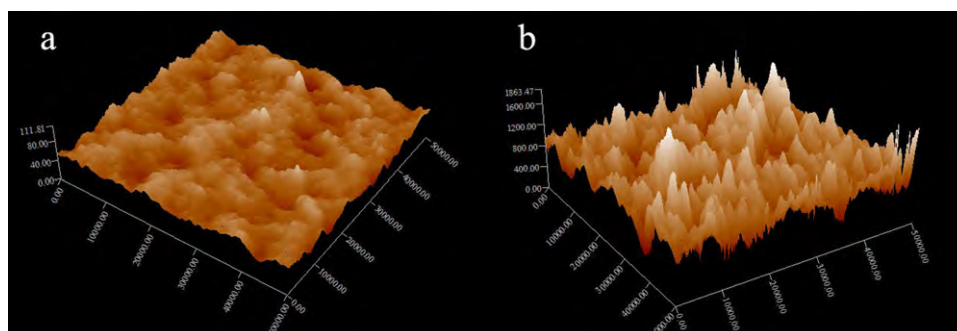


Fig. 5. AFM images of OSPA emulsion film (a) and sol–gel derived organic–inorganic hybrid film of sample 6 (b).

Table 1
Roughness parameters for samples.

Samples	Sa (Roughness Average)/nm	Sq (Root Mean Square)/nm	Sz (Ten Point Height)/nm	Sdr (Surface Area Ratio)
OSPA emulsion film	5.85	7.55	80.4	0.00612
Organic–inorganic hybrid film	156	202	1710	10.6

Table 2
Properties of organic–inorganic hybrid superhydrophobic film.

Item	Performance
Film appearance	Non-transparent, flat and white
WCA	156°
Hardness	2 H
Adhesion (grade)	2
Impact resistance	45 cm/kg
Acid resistance (3 wt% H ₂ SO ₄ , 48 h)	Film appearance no change
Alkali resistance (3 wt% NaOH, 48 h)	Film appearance no change
Salt water resistance (3 wt% NaCl, 7 days)	Film appearance no change

As can be seen from Table 2, the performance of film is good, the appearance of the film is flat and white (non-transparent), the WCA of film is 156° and the contact angle does not change with time. It indicated that the hybrid film is superhydrophobic film with good performance. The superhydrophobicity of film is attributed to nano-micro scale roughness (Fig. 6) and hydrophobic group Si–CH₃ distributed on the surface of the hybrid film. This is because the hydrolysis and the condensation of TEOS and MTES become more compatible in the double precursor system than in the sin-

gle precursor system during sol–gel process [25]. TEOS hydrolyzes and self-condenses into silica nucleus, simultaneously hydrolyzed MTES modifies the surface of silica nucleus and contributed to the formation of the double-fractal clusters. The obtained hybrid gel show weak cross-condensation between TEOS and MTES [25]. This experimental phenomenon had been confirmed in the study of hydrolysis kinetics assisted with the solid ²⁹Si MAS NMR and XPS by Xu et al. [25].

As shown in Fig. 6, there is the nano-micro scale rough structure only on the surface of the film, and the film with optimized formula is rough without porous. Inorganic SiO₂ particles inset into the polymer network of hybrid emulsion resin and waterborne primer coating, it is favor in improving the film hardness from H (waterborne primer coating) to 2 H, which makes it possible for this superhydrophobic film to be applied.

3.5. Effect of the mole ratio of MTES/TEOS

Keeping the mole ratio of (MTES+TEOS):C₂H₅OH:NH₃⁻:H₂O at 1:6:2:0.63 and the weight percentage content of OSPA

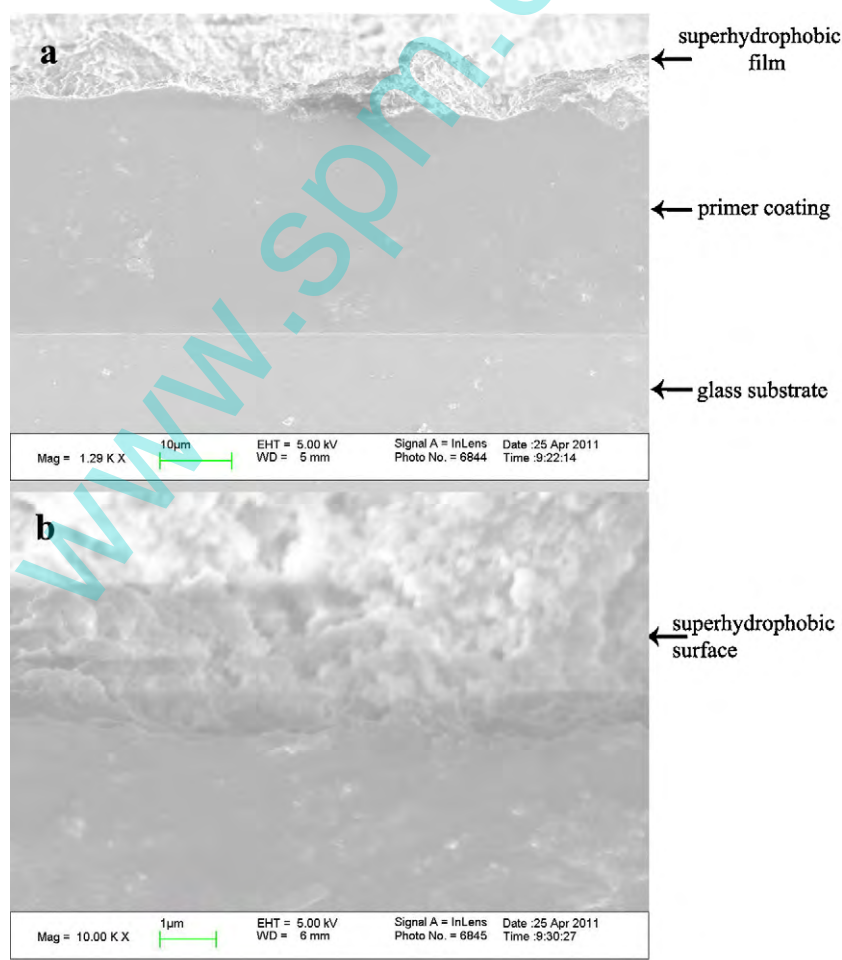
**Fig. 6.** SEM image of sol–gel derived organic–inorganic hybrid film with primer coating of sample (6), (b) is the enlarged image of (a).

Table 3
Effect of the mole ratio of MTES/TEOS on film performance.

No.	1	2	3	4	5	6	7
$n(\text{MTES})/n(\text{TEOS})$	0:1	1:4	2:3	1:1	3:2	4:1	1:0
WCA/ $^{\circ}$	–	–	–	–	145	156	131
Film appearance	pulverescent	serious cracks	more cracks	more cracks	a few cracks	flat and white	flat and white

Note: the hybrid film without primer coating.

emulsion at 25 wt%, the effect of MTES/TEOS compositions on the film performance was studied and the results are shown in Table 3. As shown in Table 3, the good film cannot be formed when the mole ratio of MTES/TEOS is below 1:1 and many cracks appear on the surface of the film. The film-forming property of sol-gel derived organic-inorganic hybrid emulsion and WCA of hybrid film are improved gradually with the increase in the mole ratio of MTES/TEOS. WCA on the hybrid film reaches the maximum 156° when the MTES/TEOS mole ratio is 4:1, and then decreases when the mole ratio of MTES/TEOS further increases. The WCA is only 131° when MTES is substituted for all of TEOS. The films keep flat and white when the MTES/TEOS mole ratio is more than 4:1.

The SEM images of the film surface of sample 5, 6 and 7 are shown in Fig. 7a–c. As can be seen from Fig. 7a, many cracks are clearly observed on film of sample 5 because of too much TEOS content. When the MTES/TEOS mole ratio is 4:1 (sample B6), the roughness structure is composed of micron aggregate of sol-gel derived silica nanoparticle with the estimated sizes around 70–90 nm (Fig. 7b). This irregular-size hierarchical structure resembles the surface of a lotus leaf. The surface morphology of sample 6 film demonstrates that dual-scale surface structure could also be constructed using these sol-gel derived organic-inorganic hybrid emulsion. Such nanoparticle-based rough surface gradually becomes smooth and WCA also is decreased as the mole ratio of MTES/TEOS continues to increase up to 1:0 from Fig. 7c. It suggests that a higher MTES/TEOS mole ratio leads to less rough surface. The above variation on the SEM images is because the reaction ratio of

hydrolysis and co-condensation of MTES and TEOS decreases with an increase in the MTES/TEOS molar ratio when ammonia is used as the catalysis [26]. Furthermore, silica nano-particles synthesized from tetra-functional TEOS sol-gel reaction generally exhibits a three-dimension microstructure with hydrophilic OH groups on the surfaces and high roughness. However, the tri-functional MTES may only have a two-dimension planar structure with hydrophobic CH_3 groups on the silica surfaces. Such variation on the surface structure would be important for obtained optimum TEOS/MTES composition to create the superhydrophobic film. Note that the SEM image of sample 1–4 could not be obtained due to the poor film quality.

3.6. Effect of the content of OSPA emulsion

Keeping the mole ratio of TEOS:MTES: $\text{C}_2\text{H}_5\text{OH}$: $\text{NH}_3\cdot\text{H}_2\text{O}$:AMP-95 at 1:4:30:10:0.63, the effect of OSPA emulsion content on the performance of the film was studied and the results are shown in Table 4.

It can be seen from Table 4 that WCA is up to 156° when the content of OSPA emulsion is 25 wt%, then decreases with the increase in the OSPA emulsion content. The film also can be formed only when the content of OSPA emulsion reaches or exceeds 25 wt% and the films are flat and white. The reason is that the main part of organic-inorganic hybrid film is inorganic network of SiO_2 , and emulsion polymer is embedded in the inorganic network when the OSPA emulsion content is low, resulting in the poor film-forming property. With the increase in

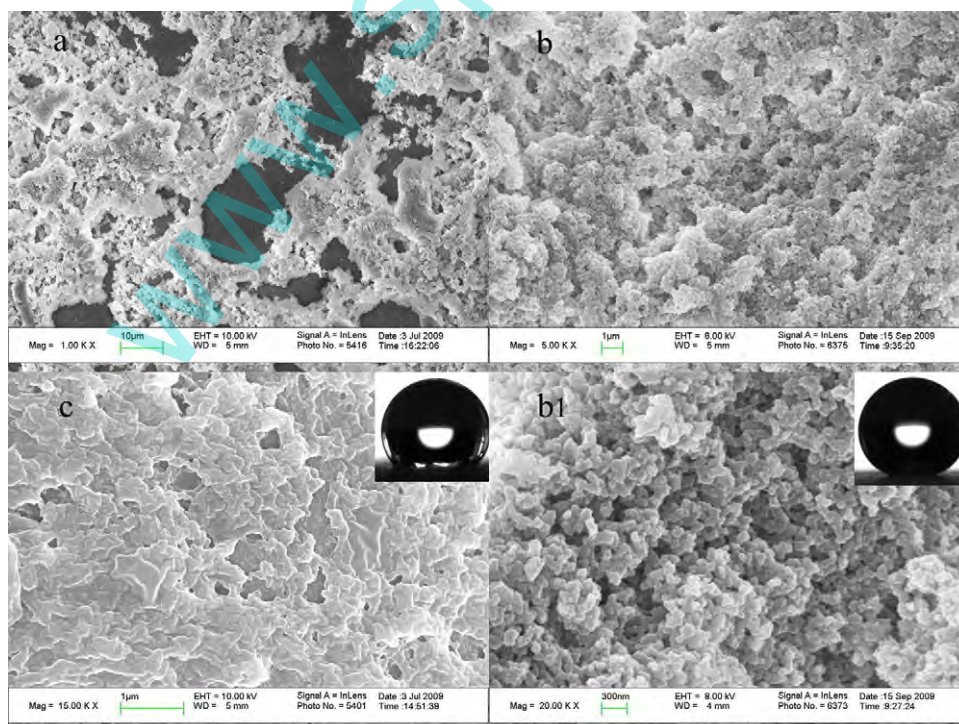


Fig. 7. SEM image and WCA of the film with different mole ratio of MTES/TEOS: (a) sample 5, (b) sample 6, and (c) sample 7. (b1) is the partial enlarged drawing of (b).

Table 4
Effect of OSPA emulsion content on film performance.

No.	8	9	10	11	12
OSPA emulsion content/%	11	17	25	29	33
WCA/°	–	152	156	154	145
Film appearance	more cracks	a few cracks	flat and white	flat and white	flat and white

Note: a, formula of sample 10 is same to that of sample 6; b, no primer coating under the hybrid film.

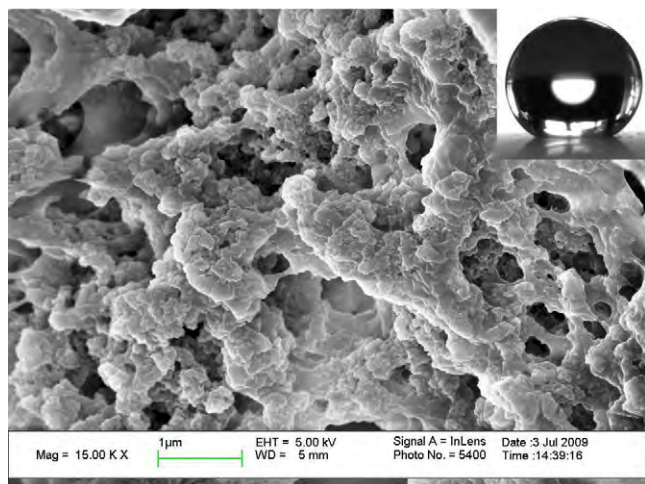


Fig. 8. SEM image of the sample 12 film with WCA of 145°.

the content of OSPA emulsion, the polymer/sol-gel derived particles interpenetrating polymer network gradually is formed and the film-forming property is improved. However the roughness and WCA are decreased with exorbitant OSPA emulsion content. In our research, the optimal content of OSPA emulsion is 25 wt%.

Figs. 8 is the SEM image and WCA of sample 12 film surface. Comparing Fig. 7b with Fig. 8, we can know that the rough structure of inorganic SiO₂ particles is filled and leveled up, roughness and hydrophobicity is decreased when the content of OSPA emulsion increases in Fig. 8.

Table 5
Effect of the mole ratio of ammonia/TEOS on film performance.

No.	13	14	15	16	17	18
$n(\text{NH}_3 \cdot \text{H}_2\text{O})/n(\text{TOES})$	0.5	2.5	5	7.5	10	12.5
WCA/°	–	–	135	145	156	150
Film appearance	serious cracks	more cracks	a few cracks	flat and white	flat and white	flat and white

Note: a, formula of sample 17 is same to that of sample 6; b, no primer coating under the hybrid film.

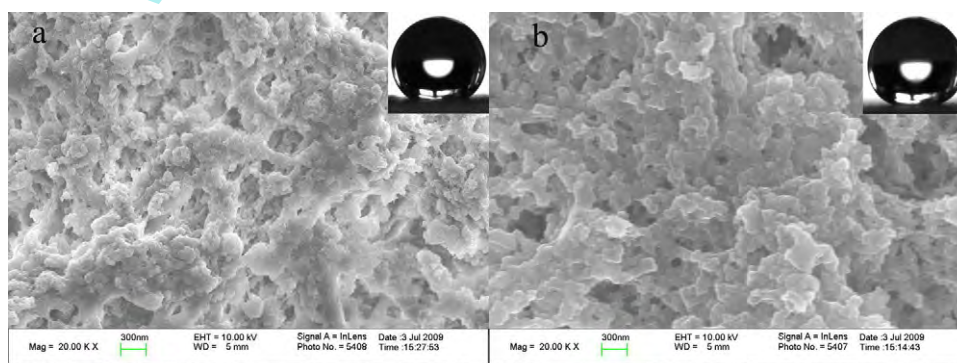


Fig. 9. SEM image and WCA of sample 16 and 18 film.

3.7. Effect of ammonia

Many different types of catalysts can be used for the preparation of silica sols [27]. Under acidic conditions, the rate of MTES hydrolysis/polymerization is much greater than that of TEOS. Under alkaline conditions, the rate of MTES hydrolysis-polymerization decreases markedly [28]. Furthermore, the rate of condensation is fast compared with that of hydrolysis in basic (pH >10) conditions. Therefore, by adjusting the alkalinity of the reaction system, the reaction ratio of hydrolysis and co-condensation can be adjusted.

Keeping the mole ratio of TEOS:MTES:C₂H₅OH:AMP-95 at 1:4:30:0.63, the content of OSPA emulsion at 25 wt%, the effect of the mole ratio of ammonia/TEOS on the film performance was studied and the results are shown in Table 5.

Table 5 shows that when the mole ratio of ammonia/TEOS reaches or exceeds 10.0, sol-gel derived organic-inorganic hybrid emulsion with the good film-forming property can be prepared and the films are flat and white. This is because organic substance/inorganic particles interpenetrating network cannot be formed due to inadequate sol-gel reaction when the content of ammonia is low, resulting that the film with good quality cannot be obtained and the amount of hydrophobic group –CH₃ also is not enough to support shifting of the character of the hybrid film from hydrophilic to superhydrophobic. With the increase in the mole ratio of ammonia, the film-forming property and hydrophobicity gradually are improved. When the mole ratio of ammonia/TEOS reached 10.0, the performance of hybrid film is optimal. At higher the mole ratio of ammonia/TEOS, the roughness and hydrophobicity decreased. WCA is 150° when the mole ratio of ammonia/TEOS is 12.5.

Fig. 9 is the SEM image and WCA of sample 16 and 18 film surfaces. Comparing Fig. 6b with Fig. 8, we can know that the film

surface becomes smooth; the rough structure of inorganic SiO₂ particles is filled and leveled up when the mole ratio of ammonia/TEOS is too low or too high (Fig. 9).

4. Conclusion

A superhydrophobic surface with remarkable film performance was obtained by spraying the hybrid emulsion on waterborne polyacrylate primer coating. The hybrid emulsion is prepared by alkaline-catalyzed co-hydrolysis and condensation reactions of TEOS, MTES and TIPVS in OSPA emulsion. TEOS and MTES derived sol-gel moieties are designed for a physical roughness and hydrophobic characteristic (Si-CH₃), OSPA emulsion is endowed for good film-forming property. When the mole ratio of MTES/TEOS reaches or exceeds 4:1, the hybrid emulsion shows remarkable film-forming property. The surface structure characterized from SEM suggests that the nanoparticle-based silica surface is observed at the mole ratio of MTES/TEOS equaling to 4:1 but change to a relatively smooth surface at a low TEOS content. The water contact angle on the hybrid film was determined to be 156°, and the contact angle hysteresis was 5° by keeping the mole ratio of TEOS:MTES:C₂H₅OH:NH₃·H₂O:AMP-95 at 1:4:30:10:0.63 and the mass percentage of OSPA emulsion at 25%. It reveals that the hybrid film exhibits super-hydrophobicity. Using this new procedure, superhydrophobic film exhibits widespread applications due to its simplicity, practicability, and low cost by non-fluorinated sol-gel derived silica materials.

Acknowledgment

We are grateful for the financial support from National Natural Science Foundation of China (Grant No. 20506005 and 21176091) and team project of Natural Science Foundation of Guangdong Province (Grant No. S2011030001366).

References

- [1] D. Öner, T.J. McCarthy, *Langmuir* 16 (2000) 7777.
- [2] R. Fürstner, W. Barthlott, C. Neinhuis, P. Walzel, *Langmuir* 21 (2005) 956.
- [3] M.H. Jin, X.J. Feng, J.M. Xi, J. Zhai, K. Cho, L. Feng, L. Jiang, *Macromol. Rapid Commun.* 26 (2005) 1805.
- [4] M.F. Wang, N. Raghunathan, B. Ziaie, *Langmuir* 23 (2007) 2300.
- [5] N. Zhao, F. Shi, Z. Wang, X. Zhang, *Langmuir* 21 (2005) 4713.
- [6] Y. Jiang, Z. Wang, X. Yu, F. Shi, H. Xu, X. Zhang, M. Smet, W. Dehaen, *Langmuir* 21 (2005) 1986.
- [7] L. Jiang, Y. Zhao, J. Zhai, *Angew. Chem. Int. Ed.* 43 (2004) 4338.
- [8] F. Shi, Z. Wang, X. Zhang, *Adv. Mater.* 8 (2005) 1005.
- [9] L. Huan, F. Lin, Z. Jin, J. Lei, Z. Daoben, *Langmuir* 20 (2004) 5659.
- [10] G. Piret, Y. Coffinier, C. Roux, O. Melnyk, R. Boukherroub, *Langmuir* 24 (2008) 1670.
- [11] J.J. Lin, C.C. Chu, M.L. Chiang, W.C. Tsai, *Adv. Mater.* 18 (2006) 3248.
- [12] L. Zhai, F.C. Cebeci, R.E. Cohen, M.F. Rubner, *Nano Lett.* 4 (2004) 1349.
- [13] C.F. Wang, Y.T. Wang, P.H. Tung, S.W. Kuo, C.H. Lin, Y.C. Sheen, F.C. Chang, *Langmuir* 22 (2006) 8289.
- [14] J. Bravo, L. Zhai, Z. Wu, R.E. Cohen, M.F. Rubner, *Langmuir* 23 (2007) 7293.
- [15] M. Hikita, K. Tanaka, T. Nakamura, T. Kajiyama, A. Takahara, *Langmuir* 21 (2005) 7299.
- [16] H.M. Shang, Y. Wang, K. Takahashi, G.Z. Cao, *J. Mater. Sci.* 40 (2005) 3587.
- [17] C.F. Wang, S.F. Chiou, F.H. Ko, C.T. Chou, H.C. Lin, C.F. Huang, F.C. Chang, *Macromol. Rapid Commun.* 27 (2006) 333.
- [18] A. Nakajima, K. Abe, K. Hashimoto, T. Watanabe, *Solid Films* 376 (2000) 140.
- [19] W. Ming, D. Wu, R. van Benthem, G. De With, *Nano Lett.* 5 (2005) 2298.
- [20] H.J. Tsai, Y.L. Lee, *Langmuir* 23 (2007) 12687.
- [21] J. Bravo, L. Zhai, Z.Z. Wu, R.E. Cohen, M.F. Rubner, *Langmuir* 23 (2007) 7293.
- [22] F. Devreux, J.P. Boilot, F. Chaput, A. Lecomte, *Phys. Rev. A* 41 (1990) 6901.
- [23] S. Dire', E. Pagani, F. Babonneau, R. Ceccato, G. Carturana, *J. Mater. Chem.* 7 (1997) 67.
- [24] Y.C. Sheen, W.H. Chang, W.C. Chen, Y.H. Chang, Y.C. Huang, F.C. Chang, *Mater. Chem. Phys.* 114 (2009) 63.
- [25] Y. Xu, R.L. Liu, D. Wu, Y.H. Sun, H.C. Gao, H.Z. Yuan, F. Deng, *J. Non-Cryst. Solids* 351 (2005) 2403.
- [26] Y. Ma, M. Kanazashi, T. Tsuru, *J. Sol-Gel Sci. Technol.* 53 (2010) 93.
- [27] A.R. Venkateswara, G.M. Pajonk, N.N. Parvathy, *J. Mater. Sci.* 29 (1994) 1807.
- [28] M.J. Van Bommel, T.N.M. Bernards, A.H. Boonstra, *J. Non-Cryst. Solids* 128 (1991) 231.